Uniform damping control: discretization and optimization

Larry Silverberg, James M. Redmond, and Leslie L. Weaver Jr.

Mars Mission Research Center, North Carolina State University, Raleigh, NC, USA

This paper develops the control discretization and control optimization processes for the uniform damping of structures. A distributed uniform damping control is first shown to represent a first-order approximation to an associated globally optimal solution. This approximation is shown to be accurate for moderate to low levels of damping. The implementation of uniform damping control with discrete control forces is then demonstrated, using a subdomain approach, whereby a transformation of coordinates is carried out and a resulting subdomain polynomial expansion is truncated. Control laws are developed for one, two, and three discrete control forces per subdomain. Next, a steepest descent method is developed for the optimal assignment of control gains and the locations of the control forces. As a general rule the number of modes that can be uniformly damped is twice the number of control forces. The control discretization and associated optimization processes are illustrated via the control of a cantilever beam.

Keywords: uniform damping, control, discretization, optimization

Introduction

Over the past few decades the drive toward more flexible structures has led to the development of control methods for flexible structures. These methods, often referred to as *structural control methods*, are designed to control the previously unimportant structural modes. Furthermore, they find a strong connection between the associated structural and control parameters for the purpose of rendering an efficient design process.

Within the context of structural control we can distinguish between *mode preserving control* and *mode coupling control*. Mode preserving control methods are based on the desire, in closing the loop, to preserve the structural modes. That is, we let the natural structural modes (associated with the uncontrolled structure) and the closed-loop structural modes (associated with the controlled structure) be identical to each other. Mode preserving control is used when a sufficient number of control inputs is available to independently control the structural modes, which is generally the case when the number of control inputs is of the order of the number of controlled modes. In contrast, when significantly fewer control inputs than controlled modes are available, a mode coupling control method is adopted.

Address reprint requests to Prof. Silverberg at the Mars Mission Research Center, North Carolina State University, Raleigh, NC 27695-7910, USA.

Received 10 April 1991; revised 16 September 1991; accepted 10 October 1991

Mode preserving control is also referred to as *natural control* because the structure's natural characteristics are preserved. The objective to preserve the modes was first demonstrated when natural control was shown to provide a globally optimal solution to the control problem.[1] Later, the desire to preserve the natural frequencies was exposed. It was shown that the fuel (or power) consumed in a mode preserving control system is minimized when we let the closed-loop frequencies of oscillation be identical to the natural frequencies of oscillation, that is, when we preserve the natural frequencies.[2] An exception to this occurs when the structure is subject to a persistent harmonic excitation, in which case the interest lies in appropriately shifting the natural frequencies. Another property associated with both mode preserving control and mode coupling control lies in the objective to uniformly dampen the motion. For mode preserving control it was shown both that fuel is minimized and that the presence of lingering vibration associated with one mode damping out slower than the others is avoided when the natural modes are uniformly damped.[3]

To summarize the previous remarks, when a sufficient number of control inputs is available, an attractive system performance is achieved provided that (a) the natural modes are preserved, (b) the natural frequencies are preserved, and (c) the modes are uniformly damped. Furthermore, the associated control law becomes decentralized, and the control gains become proportional to the structure's mass distribution and independent of its stiffness.

In its purest form the previously described uniform

damping control is achieved by using distributed forces. However, implementation commonly precludes the use of distributed forces, leaving spatially discrete control forces as the only alternative. Ultimately, the performance of the control system is dictated by the process by which the control law employing distributed forces is converted into a form suitable for use with discrete control forces. This process requires *control discretization* and *control optimization*. The effectiveness of the control discretization and optimization processes depend on three types of parameters: (a) the number of discrete control forces, (b) the locations of the discrete control forces, and (c) the control gains.

As mentioned earlier, the distributed uniform damping forces are governed by a decentralized control law. In selecting a control discretization process the question arises how to preserve the decentralized nature of the control law. As a candidate a global function approach such as the Rayleigh-Ritz method must be ruled out since the discretized control laws would no longer be decentralized. Instead we consider a discretization method which preserves the decentralized nature of the control law.

A uniform damping control discretization process is described later in this paper. The process begins by dividing the structure into subdomains, each containing discrete control forces. Within each subdomain the displacements are expressed in series as a linear combination of space-dependent functions. The truncation of this series leads to discrete control laws. As described in a later section, we let the number of discrete forces in a given subdomain be equal to the number of terms retained in the truncated series, and we obtain the decentralized control laws. These results are applied to one-dimensional structures in the following section. Next, an optimization of the uniform damping control gains and the actuator locations is developed, using a steepest descent method. As a general rule it is shown that twice the number of control forces is equal to the number of modes that can be uniformly damped.

The previously described control discretization and control optimization processes are applied to one-dimensional structures, and a quantitative analysis compares the results in the section on numerical illustrations. The one-dimensional structures represent the most elementary structural components and perhaps the clearest way to demonstrate the control discretization and optimization processes and their effects. Finally, a summary of the paper is given.

Distributed control forces

The equation governing the motion of a flexible structure is represented by

$$m(P)\ddot{u}(P,t) = -Lu(P,t) + f(P,t) \tag{1}$$

with $m(P)$ = structure's mass density at point P
$u(P, t)$ = displacement at point P at time t
L = differential operator* representing the structure's stiffness
$f(P, t)$ = the external control force acting at point P at time t

Active control of such a structure involves generating an external control force $f(P, t)$ to accomplish vibration suppression or to maneuver the structure. This paper is concerned with vibration suppression via feedback control. Accordingly, the external control force is governed by a feedback control law, expressed in the functional form

$$f(P,t) = Gu(P,t) + H\dot{u}(P,t) \tag{2}$$

where G and H are linear control gain operators.

Within the context of linear optimal control a performance functional can be defined as the integral over time of the sum of the total (potential and kinetic) energy and the fuel consumed by the control force. This leads to the globally† optimal control force governed by (2) in which G and H become[1]

$$G(\ ) = \sum_{r=1}^{\infty} g_r m(P)\phi_r(P) \int_D m(P)\phi_r(P)(\ )\,dD$$

$$H(\ ) = \sum_{r=1}^{\infty} h_r m(P)\phi_r(P) \int_D m(P)\phi_r(P)(\ )\,dD \tag{3}$$

(4)

where

$$g_r = \omega_r^2 - \omega_r(\omega_r^2 + 2\alpha^2)^{1/2} \tag{5a}$$

$$h_r = -[-2\omega_r^2 + 2\alpha^2 + 2\omega_r(\omega_r^2 + \alpha^2)^{1/2}]^{1/2} \tag{5b}$$

with ϕ_r = rth natural mode of vibration
g_r = rth modal displacement control gain
h_r = rth modal velocity control gain
ω_r = rth natural frequency of oscillation
α = optimization parameter

Globally optimal control has been shown to be a natural control.[1] Therefore the natural modes of vibration are preserved in the presence of the feedback control system. Equations (4) and (5) are the modal decompositions of the operators G and H**. A first-order Taylor series approximation of (5a) and (5b) for $\alpha < \omega_r$ with the approximation

$$(\omega_r^2 + 2\alpha^2)^{1/2} = \omega_r + \frac{\alpha^2}{\omega_r}$$

yields the familiar uniform damping modal control gains,

$$g_r = -\alpha^2 \tag{6a}$$

$$h_r = -2\alpha \tag{6b}$$

---

* L is self-adjoint and positive (semi-) definite, implying that its eigenfunctions are real and its associated eigenvalues are positive (or zero).

† The term "global" refers to an optimization allowing for unconstrained distributed forces.

** g_r and h_r are the associated eigenvalues of G and H, respectively.

in which the optimization parameter α is now recognized as a uniform damping rate. Substituting (6a) and (6b) into (2) and (3) yields the distributed uniform damping control law.[3]

$$f(P,t) = -\alpha^2 m(P)u(P,t) - 2\alpha m(P)\dot{u}(P,t) \quad (7)$$

The quality of the approximation of globally optimal control by uniform damping control depends on the accuracy of the Taylor series approximation. *Figure 1* compares uniform damping control (UDC) and the globally optimal control (GOC) solutions. Specifically, the closed-loop frequencies associated with GOC, denoted by β_r, and the closed-loop frequencies associated with UDC, which are identical to the natural frequencies, are compared. The normalized closed-loop frequencies (β_r/ω_r) are expressed as a function of the normalized damping rates (α_r/ω_r). As shown, for $\alpha_r/\omega_r < 0.4$ (40% damping) the difference between the normalized closed-loop frequencies is less than 0.5%.

Subdomain function expansions

In the previous section, uniform damping control was shown to provide an accurate approximation of globally optimal control for moderate levels of damping. The development led to the uniform damping control law given by (7) in which the forces are distributed. Toward discretizing the control law we perform a transformation of coordinates as follows:

The structure is divided into N subdomains D_r ($r = 1, 2, \ldots, N$). Next the displacement in D_r can be expressed as an infinite sum of space dependent functions multiplied by time dependent coefficients as

$$u(P,t) = p_{r1}(P)a_{r1}(t) + p_{r2}(P)a_{r2}(t) + p_{r3}(P)a_{r3}(t) + \ldots \quad (8)$$

in which

$$a_{rs}(t) = \int_{D_r} m(P)p_{rs}(P)u(P,t)\,dD \quad (9)$$

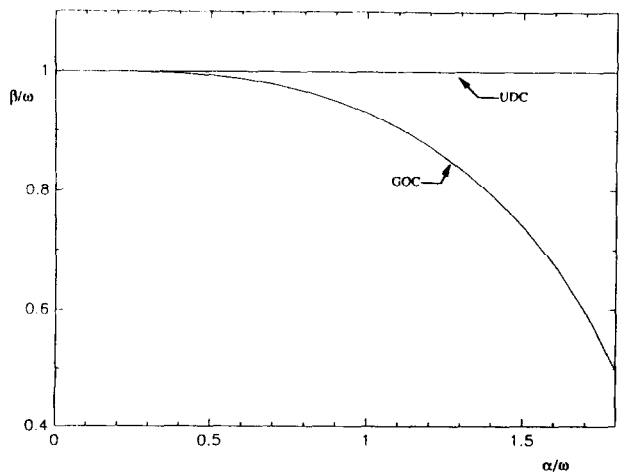

Figure 1. Closed-loop frequency versus decay rate for the globally optimal and uniform damping solutions

with $a_{rs}(t)$ = sth time dependent displacement coefficient in D_r
$p_{rs}(P)$ = sth space dependent function defined over D_r

For convenience the space dependent functions selected are mutually orthogonal and normalized with respect to the mass density, that is,

$$\int_{D_r} m(P)p_{rs}(P)p_{rt}(P)\,dD = \delta_{st} \quad (10)$$

Then the distributed control force in D_r can be expressed as

$$f(P,t) = m(P)p_{r1}(P)A_{r1}(t) + m(P)p_{r2}(P)A_{r2}(t) + \ldots \quad (11)$$

in which

$$A_{rs}(t) = \int_{D_r} p_{rs}(P)f(P,t)\,dD \quad (12)$$

with $A_{rs}(t)$ the sth time dependent force coefficient in D_r.

Substituting (8–12) into (7) yields the subdomain control laws,

$$A_{rs}(t) = -\alpha^2 a_{rs}(t) - 2\alpha\dot{a}_{rs}(t) \quad (r = 1,2,\ldots,N, s = 1,2,\ldots) \quad (13)$$

The subdomain control laws (13) are equivalent to the distributed uniform damping control law (7) in which the displacements and forces (u and f) have been replaced by a_{rs} and A_{rs}, respectively, through the transformation of coordinates (8) and (11).

Discrete control forces

Expressing the subdomain displacements in series in (8) enabled us to examine the control law within a given subdomain. The control law is now discretized by simply truncating the infinite series in (8). We obtain in D_r

$$u(P,t) = p_{r1}(P)a_{r1}(t) + p_{r2}(P)a_{r2}(t) + \ldots + p_{rn}(P)a_{rn}(t) \quad (14)$$

Letting $u(P_{rs}, t)$, ($s = 1, 2, \ldots, n$) represent spatially discrete measurements in D_r, we obtain from (14)

$$U_r(t) = P_r a_r(t) \quad (15)$$

in which

$$U_r(t) = [u(P_{r1},t), u(P_{r2},t), \ldots, u(P_{rn},t)]^T$$

$$P_r = [p_{rs}(P_{rt})]^T$$

$$a_r(t) = [a_{r1}(t), a_{r2}(t), \ldots, a_{rn}(t)]^T$$

The distributed control force in the rth subdomain is now represented by discrete control forces as

$$f_r(P,t) = f_{r1}(t)\delta(P - P_{r1}) + f_{r2}(t)\delta(P - P_{r2}) + \ldots + f_{rn}(t)\delta(P - P_{rn}) \quad (16)$$

in which we select the same number of discrete control forces in a given subdomain as space dependent functions. It turns out that no advantage is gained by selecting different numbers of discrete control forces and space dependent functions. Substituting (16) into (12),

$$A_{rs}(t) = p_{rs}(P_{r1})f_{r1}(t) + p_{rs}(P_{r2})f_{r2}(t) + \ldots + p_{rs}(P_{rn})f_{rn}(t) \quad (17)$$

or, in matrix form,

$$A_r(t) = P_r^T F_r(t) \quad (18)$$

in which

$$A_r(t) = [A_{r1}(t), A_{r2}(t), \ldots, A_{rn}(t)]^T$$

$$F_r(t) = [f_{r1}(t), f_{r2}(t), \ldots, f_{rn}(t)]^T$$

Finally, substituting (15) and (18) into (13) for $s = 1, 2, \ldots, n$, we obtain the discretized uniform damping control law,

$$F_r(t) = -\alpha^2 M_r U_r(t) - 2\alpha M_r \dot{U}_r(t) \quad (19)$$

where

$$M_r = P_r^{-T} P_r^{-1} \quad (20)$$

with M_r the subdomain mass matrix.

Application to one-dimensional structures

Let us now consider structures composed of one-dimensional subdomains. We approximate the subdomain displacement by orthogonal polynomial functions; the first three are given by

$$p_{r1} = m_r^{-1/2} \quad (21a)$$

$$p_{r2} = I_r^{-1/2}\xi_r \quad (21b)$$

$$p_{r3} = J_r^{-1/2}\left(\xi_r^2 - \frac{1}{12}\right) \quad (21c)$$

where

$$m_r = \int_{D_r} m(\xi_r)\, d\xi_r \quad (22a)$$

$$I_r = \int_{D_r} m(\xi_r)\xi_r^2\, d\xi_r \quad (22b)$$

$$J_r = \int_{D_r} m(\xi_r)\left(\xi_r^2 - \frac{1}{12}\right)^2 d\xi_r \quad (22c)$$

with m_r = subdomain mass
I_r = subdomain mass moment of inertia
J_r = subdomain mass moment of curvature
ξ_r = nondimensional subdomain coordinate ranging from -0.5 to 0.5

The orthogonal polynomial functions are recognized as Legendre polynomials weighted by the mass per unit length so that $\int_{D_r} m(\xi_r)p_{ri}(\xi_r)p_{rj}(\xi_r)\, d\xi_r = \delta ij$. The Legendre polynomials (with mass per unit length of 1) are shown in *Figure 2*.

The number of polynomial functions per subdomain influences the control discretization process. The following examines the control discretization process

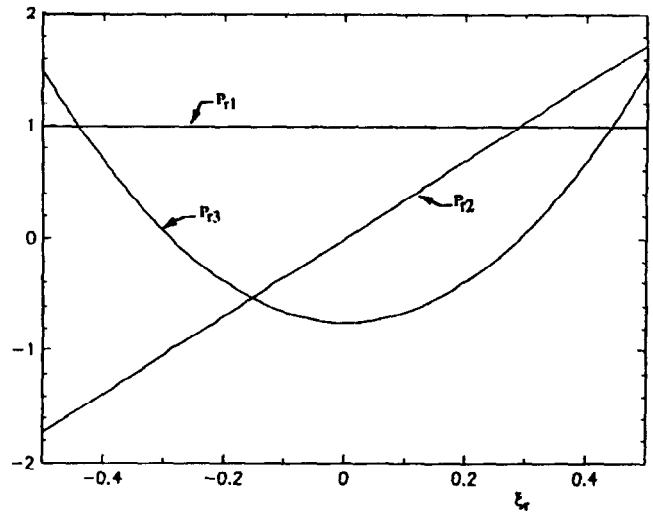

Figure 2. Orthogonal polynomial functions

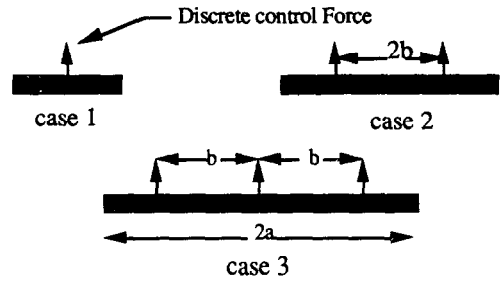

Figure 3. Subdomains with one, two, and three discrete control forces

using different numbers of polynomial functions. The subdomains defined for each case are shown in *Figure 3*.

Case 1: One discrete control force per subdomain (n = *1*)

The structure is divided into subdomains, each containing only one discrete control force. Thus only one polynomial function is considered in (14). From (15), (20), and (21),

$$P_r = [m_r^{-1/2}] \quad (23a)$$

$$M_r = [m_r] \quad (23b)$$

Case 2: Two discrete control forces per subdomain (n = *2*)

The structure is divided into subdomains, each containing two discrete control forces. Two polynomial functions are considered in (14). From (15), (20), and (21),

$$P_r = \begin{bmatrix} m_r^{-1/2} & -I_r^{-1/2}b \\ m_r^{-1/2} & I_r^{-1/2}b \end{bmatrix} \quad (24a)$$

$$M_r = \frac{1}{4b^2}\begin{bmatrix} m_r b^2 + I_r & m_r b^2 - I_r \\ m_r b^2 - I_r & m_r b^2 + I_r \end{bmatrix} \quad (24b)$$

Case 3: Three discrete control forces per subdomain (n = 3)

The structure is divided into subdomains, each containing three discrete control forces. Three polynomial functions are considered in (14). From (15), (20), and (21),

$$P_r = \begin{bmatrix} m_r^{-1/2} & -I_r^{-1/2}b & J_r^{-1/2} & \left(b^2 - \frac{1}{3}a^2\right) \\ m_r^{-1/2} & 0 & & -J_r^{-1/2}\frac{1}{3}a^2 \\ m_r^{-1/2} & I_r^{-1/2}b & J_r^{-1/2} & \left(b^2 - \frac{1}{3}a^2\right) \end{bmatrix} \tag{25a}$$

$$M_r = \begin{bmatrix} \left(\frac{a^2}{6b^2}\right)^2 m_r + \frac{1}{4b^2}I_r + \frac{1}{4b^4}J_r & & \text{sym} \\ \frac{a^2\left(b^2 - \frac{a^2}{3}\right)}{6b^4}m_r - \frac{1}{4b^4}J_r & \frac{\left(b^2 - \frac{a^2}{3}\right)^2}{b^4}m_r + \frac{1}{b^4}J_r & \\ \left(\frac{a^2}{6b^2}\right)^2 m_r - \frac{1}{4b^2}I_r + \frac{1}{4b^4}J_r & \frac{a^2\left(b^2 - \frac{a^2}{3}\right)}{6b^4}m_r - \frac{1}{4b^4}J_r & \left(\frac{a^2}{6b^2}\right)^2 m_r + \frac{1}{4b^2}I_r + \frac{1}{4b^4}J_r \end{bmatrix} \tag{25b}$$

Uniform damping control optimization

The control discretization process, as described in the previous section, determines control gains for a prescribed set of control force locations. Indeed, the quality of the control discretization processes was compared independent of the location of the control forces. A quantitative comparison of the three cases shown in *Figure 3* is illustrated later in which the actuator locations are identical for the cases considered.

For now we consider case 1 of the control discretization process and proceed with the optimal assignment of control gains and of control force locations. Substituting (23b) into the scalar discretized uniform damping control law (19), we obtain

$$F_r = -\alpha^2 m_r U_r - \alpha^2 m_r \dot{U}_r \tag{26}$$

where F_r and U_r are now scalar quantities, N denotes the number of subdomains, and $U_r = u(P_r, t)$ are located at the points P_r. Whereas the closed-loop frequencies are identical to the natural frequencies and the modes are uniformly damped when the control force is distributed, the use of (26) yields closed-loop eigenvalues, given by

$$\lambda_{Cr} = -\alpha_r + i\beta_r \tag{27}$$

with λ_{Cr} = rth closed-loop eigenvalue
α_r = rth modal decay rate
β_r = rth closed-loop frequency of oscillation

As indicated in (27), the closed-loop eigenvalues shift, that is, $\lambda_{cr} \neq -\alpha + i\omega_r$. The purpose of the optimization is to prevent this shift in a subset of modes, in which case a subset of the closed-loop eigenvalues is given by $\lambda_{cr} = -\alpha + i\omega_r$. The optimization proceeds by appropriately varying the subdomain masses $m_r(r = 1, 2, \ldots, N)$ and the control force locations $P_r(r = 1, 2, \ldots, N)$. To a first-order approximation,

$$\delta\alpha_r = \sum_{s=1}^{N} \frac{\partial\alpha_r}{\partial m_s}\delta m_s + \sum_{s=1}^{N} \frac{\partial\alpha_r}{\partial P_s}\delta P_s \qquad (r = 1, 2, \ldots, M) \tag{28}$$

with $\delta(\ )$ = variation of given quantities
M = number of optimized modes

The variations of m_s and P_s can be selected simply on the basis of a steepest descent method,[4] in which

$$\delta m_s = -h\frac{\partial\alpha_r}{\partial m_s} \qquad \delta P_s = -h\frac{\partial\alpha_r}{\partial P_s} \qquad (s = 1, 2, \ldots, M) \tag{29}$$

with h the step size.

The derivatives $\partial\alpha_r/\partial m_s$ and $\partial\alpha_r/\partial P_s$ in (29) can be either obtained exactly[5] or approximated by neglecting the small differences between the closed-loop modes of vibration and the natural modes of vibration, to first obtain[3]

$$\alpha_r = \alpha\sum_{s=1}^{N} m_s\phi_r^2(P_s) \tag{30a}$$

$$\beta_r = \omega_r\left[1 + \frac{1}{2}\left(\frac{\alpha_r}{\omega_r}\right)^2\left(1 - \sum_{s=1}^{N} m_s\phi_r^2(P_s)\right)\right] \tag{30b}$$

Then, differentiating (30a) with respect to m_s and P_s, we obtain

$$\frac{\partial\alpha_r}{\partial m_s} = \alpha\phi_r^2(P_s) \qquad \frac{\partial\alpha_r}{\partial P_s} = 2\alpha m_s\phi_r(P_s)\frac{\partial\phi_r}{\partial P}(P_s) \tag{31}$$

The index r, indicating which eigenvalue to shift, is selected as the index corresponding to the maximum

difference between the rth decay rate and the desired decay rate α, that is, corresponding to max $|\alpha - \alpha_r|$. The step size h is chosen to eliminate the error $|\alpha - \alpha_r|$ and then repeated for each r. Note that eliminating the error in the rth decay rate causes the other $M - 1$ decay rates to change. Therefore this process is iterative. Also note from (30b), as the decay rates α_r converge to the desired decay rate α, that the closed-loop frequencies naturally converge to the natural frequencies.

Numerical illustration

For illustrative purposes we consider a cantilever beam of unit length ($L = 1$) and unit mass per unit length ($m = 1$) undergoing bending vibration. The associated stiffness operator is given by $L = 0.01\ (\partial^4/\partial x^4)$. The beam is subject to the boundary conditions $u = \partial u/\partial x = 0$ at $x = 0$ and $d^2u/\partial x^2 = \partial^3 u/\partial x^3 = 0$ at $x = L$. We select a uniform decay rate given by $\alpha = 0.2$. Ten modes were assumed to participate in the system response. *Table 1* lists the lowest 10 natural frequencies of the beam.

The beam is divided into subdomains in three different ways as shown in *Figure 4*. In all cases the beam is controlled by six evenly spaced discrete control forces. This system readily lends itself to subdomain divisions containing one, two, and three control forces. For case 1 we select six subdomains with one control force per subdomain. Three subdomains, each containing two discrete control forces, and two subdomains, each with three discrete control forces, represent cases 2 and 3, respectively.

The closed-loop eigenvalues for globally optimal control, distributed uniform damping control, and discrete uniform damping control obtained by the three control discretization processes are given in *Table 2*. As indicated in *Table 2*, the distributed uniform damping control eigenvalues closely approximate the globally optimal eigenvalues. As expected, each of the discretized cases yields a deterioration in the eigenvalues due to the use of discrete actuators.

Figure 5 shows the response of the beam tip to an initial impulse of magnitude 0.1 imparted at $x = \frac{3}{4}L$.

Table 1. Ten lowest natural frequencies (rad/sec)

1	0.3516
2	2.2034
3	6.1697
4	12.0902
5	19.9860
6	29.8556
7	41.6991
8	55.5165
9	71.3079
10	89.0732

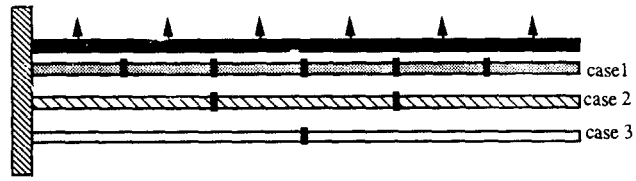

Figure 4. Division of uniform cantilever beam into subdomains

Table 2. Ten lowest closed-loop eigenvalues (rad/sec) for globally optimal control, distributed uniform damping, and cases 1–3

	Distributed solutions	
	GOC	UDC
1	$-0.1937 \pm 0.3481i$	$-0.2000 \pm 0.3516i$
2	$-0.1998 \pm 2.2034i$	$-0.2000 \pm 2.2034i$
3	$-0.2000 \pm 6.1697i$	$-0.2000 \pm 6.1697i$
4	$-0.2000 \pm 12.0902i$	$-0.2000 \pm 12.0902i$
5	$-0.2000 \pm 19.9860i$	$-0.2000 \pm 19.9860i$
6	$-0.2000 \pm 29.8556i$	$-0.2000 \pm 29.8556i$
7	$-0.2000 \pm 41.6991i$	$-0.2000 \pm 41.6991i$
8	$-0.2001 \pm 55.5165i$	$-0.2000 \pm 55.5165i$
9	$-0.2000 \pm 71.3079i$	$-0.2000 \pm 71.3079i$
10	$-0.2002 \pm 89.0732i$	$-0.2000 \pm 89.0732i$

	Discrete solutions		
	Case 1	Case 2	Case 3
1	$-0.1975 \pm 0.3523i$	$-0.1996 \pm 0.3517i$	$-0.2001 \pm 0.3516i$
2	$-0.1911 \pm 2.2039i$	$-0.2061 \pm 2.2032i$	$-0.2072 \pm 2.2032i$
3	$-0.1849 \pm 6.1700i$	$-0.2277 \pm 6.1694i$	$-0.2151 \pm 6.1697i$
4	$-0.1764 \pm 12.0905i$	$-0.1917 \pm 12.0906i$	$-0.2988 \pm 12.0901i$
5	$-0.1592 \pm 19.9866i$	$-0.1980 \pm 19.9868i$	$-0.2174 \pm 19.9879i$
6	$-0.0750 \pm 29.8559i$	$-0.0974 \pm 29.8561i$	$-0.1370 \pm 29.8562i$
7	$-0.3310 \pm 41.6974i$	$-0.4406 \pm 41.6958i$	$-0.6765 \pm 41.6906i$
8	$-0.2485 \pm 55.5148i$	$-0.3245 \pm 55.5155i$	$-0.4982 \pm 55.5082i$
9	$-0.2353 \pm 71.3066i$	$-0.3053 \pm 71.3079i$	$-0.2819 \pm 71.3056i$
10	$-0.2350 \pm 89.0721i$	$-0.2433 \pm 89.0719i$	$-0.2656 \pm 89.0718i$

Only slight differences can be perceived among the responses. However, each of the discrete cases is characterized by a lingering high-frequency mode. This effect is attributed to the presence of a relatively low decay rate associated with the sixth mode in each of the discrete cases. A marginal advantage is gained by using multiple actuators per subdomain in that the severity of this effect is reduced.

Among the discrete cases, using one, two, and three control forces per subdomain yields comparable results. Therefore the simplest approach to discretization, using one actuator per subdomain, would be adequate under usual circumstances.

The steepest descent algorithm for uniform damping control optimization is then employed for case 1. The objective is to uniformly dampen the first 10 natural modes of vibration. As shown in *Table 3*, convergence to uniform damping is obtained in six iterations. Furthermore, the closed-loop frequencies naturally converge to the natural frequencies as we predicted in the previous section.

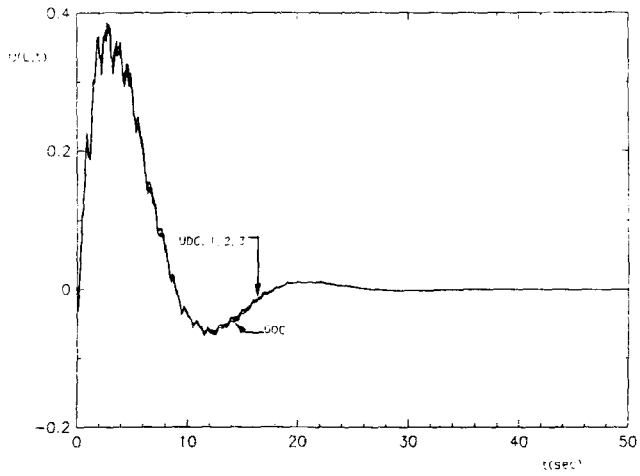

Figure 5. Tip displacement for beam controlled using globally optimal, distributed uniform damping, cases 1, 2, and 3

Conclusions

This paper has shown how to uniformly dampen the motion of structures using discrete control forces. Toward that end the control discretization and control optimization processes for uniform damping of structures were developed. The associated distributed uniform damping solution was shown to be a close approximation to the globally optimal solution when the designer decay rate normalized with respect to the natural frequency is less than 0.4. Three different control discretization strategies were developed. The examination of the control discretization processes revealed that the scalar form of the discretized control law (equation (26)) closely approximates distributed control, thereby countering the need for higher order discretized control laws. The optimal assignment of control gains and actuator locations was then developed, using a steepest descent method. In the optimization process, convergence to uniform damping rates was shown to naturally guarantee convergence of the closed-

Table 3. Uniform damping convergence

	Iteration no.					
	1	2	3	4	5	6
			Eigenvalue convergence			
λ_1	$-0.183 \pm i0.3562$	$-0.177 \pm i0.3573$	$-0.202 \pm i0.3510$	-0.201 ± 0.3515	$-0.200 \pm i0.3517$	-0.200 ± 0.3517
λ_2	$-0.189 \pm i2.2028$	$-0.183 \pm i2.2043$	$-0.199 \pm i2.2036$	$-0.199 \pm i2.2035$	$-0.200 \pm i2.2034$	$-0.200 \pm i2.2035$
λ_3	$-0.186 \pm i6.1693$	$-0.182 \pm i6.1701$	$-0.209 \pm i6.1698$	$-0.204 \pm i6.1699$	$-0.201 \pm i6.1699$	$-0.200 \pm i6.1699$
λ_4	$-0.184 \pm i12.090$	$-0.160 \pm i12.091$	$-0.206 \pm i12.091$	$-0.203 \pm i12.091$	$-0.200 \pm i12.091$	$-0.200 \pm i12.091$
λ_5	$-0.184 \pm i19.986$	$-0.194 \pm i19.984$	$-0.187 \pm i19.983$	$-0.194 \pm i19.983$	$-0.199 \pm i19.983$	$-0.200 \pm i19.983$
λ_6	$-0.214 \pm i29.856$	$-0.139 \pm i29.855$	$-0.199 \pm i29.854$	$-0.201 \pm i29.854$	$-0.200 \pm i29.854$	-0.200 ± 29.854
λ_7	$-0.365 \pm i41.698$	$-0.200 \pm i41.699$	$-0.200 \pm i41.699$	$-0.200 \pm i41.699$	$-0.200 \pm i41.699$	$-0.200 \pm i41.699$
λ_8	$-0.153 \pm i55.515$	$-0.170 \pm i55.516$	$-0.202 \pm i55.516$	$-0.201 \pm i55.516$	$-0.200 \pm i55.516$	$-0.200 \pm i55.516$
λ_9	$-0.195 \pm i71.307$	$-0.266 \pm i71.307$	$-0.204 \pm i71.308$	$-0.203 \pm i71.308$	$-0.200 \pm i71.308$	$-0.200 \pm i71.308$
λ_{10}	$-0.183 \pm i89.072$	$-0.174 \pm i89.072$	$-0.200 \pm i89.071$	$-0.201 \pm i89.071$	$-0.200 \pm i89.071$	$-0.200 \pm i89.071$
			Actuator placement			
x_1	0.12035	0.11823	0.14337	0.14653	0.14726	0.14704
x_2	0.27654	0.21761	0.23209	0.23371	0.23424	0.23403
x_3	0.42656	0.43087	0.46414	0.46367	0.46289	0.46287
x_4	0.57351	0.59340	0.60657	0.60660	0.60665	0.60664
x_5	0.72268	0.68337	0.69287	0.69080	0.68952	0.68962
x_6	0.88436	0.92546	0.92025	0.91737	0.91696	0.91715
			Region mass gain			
m_1	0.17464	0.14245	0.16555	0.17254	0.17774	0.17830
m_2	0.16851	0.16587	0.17699	0.16599	0.15827	0.15771
m_3	0.16689	0.13612	0.15028	0.15115	0.15139	0.15136
m_4	0.16689	0.13637	0.14981	0.15892	0.16764	0.16823
m_5	0.16870	0.15381	0.18138	0.17388	0.16507	0.16421
m_6	0.16924	0.16549	0.18131	0.18150	0.18226	0.18261

loop frequencies to the natural frequencies. As a numerical example, six discrete control gains and locations were optimally assigned to uniformly damp 10 modes of vibration. As a rule of thumb, twice the number of modes as control forces can be uniformly damped.

Acknowledgment

This research is supported in part by NASA grant NAGW-1331 to the Mars Mission Research Center.

References

1 Meirovitch, L. and Silverberg, L. M. Globally optimal control of self-adjoint distributed systems. *J. Optim. Control Appl. Meth.* 1983, **4**, 365–386

2 Silverberg, L. M. and Morton, M. H. On the nature of natural control. *J. Vib. Acoust., Stress Reliab. Des.* 1989, **111**, 412–422

3 Silverberg, L. M. Uniform damping control of spacecraft. *J. Guid. Control Dyn.* 1986, **9**, 221–227

4 Taylor, A. E. and Mann, W. R. *Advanced Calculus*, John Wiley, New York, 1983

5 Lim, K. B., Junkins, J. L., and Wang, B. P. A Re-examination of eigenvector derivatives. *J. Guid. Control Dyn.* 1987, **10**, 581–587